Available online at www.sciencedirect.com
ScienceDirect
Journal of the European Ceramic Society 31 (2011) 3011–3020
www.elsevier.com/locate/jeurceramsoc

High performance environmental barrier coatings, Part II: Active filler loaded SiOC system for superalloys

Kaishi Wang [a], Martin Günthner [b], Günter Motz [b], Rajendra K. Bordia [a,*]

[a] University of Washington, Department of Materials Science and Engineering, Seattle, WA 98195-2120, USA
[b] University of Bayreuth, Ceramic Materials Engineering (CME), D-95440 Bayreuth, Germany

Received 2 March 2011; received in revised form 23 May 2011; accepted 31 May 2011
Available online 13 July 2011

Abstract

Polymer derived ceramic (PDC) matrix composite coatings are a promising candidate to be used as alternative environmental barrier coatings, such as in oxidation protection. This paper reports the processing of three PDC coating systems on a superalloy substrate, Inconel 617, using a simple dip coating method. The performance of SiON coating, particle filled SiOC coating, and their combined coating system is evaluated by long time static oxidation testing at 800 °C for 100–200 h. Two key parameters have been analyzed: the weight gain of the coating samples and the thickness of the thermally grown oxide (TGO) layer at the ceramic–metal interface. Results show that all three coating systems are able to significantly reduce the weight gain of metal substrates due to oxidation. However, the SiON bond coat + particle filled SiOC top coat double-layer coating system is most effective in maintaining the integrity of the substrate in the investigated 200 h. Based on the kinetics of oxidation, likely rate controlling steps are identified.

Keywords: Polymer derived ceramics; Composites; Interfaces; Structural applications; Failure analysis

1. Introduction

Ceramic coatings play an important role in providing structural or environmental protection and functionality to a system. Commercially, expensive vapour phase techniques, like PVD and CVD, are used to deposit single or multi-elemental ceramic materials, for instance, those used in gas turbines. In contrast, a large number of preceramic polymers are liquid or soluble so that low-cost alternatives such as dip-coating, spray-coating and spin-coating can be utilized to deposit polymers or their solutions onto substrates, which can then be converted to ceramic coating materials. And since the polymer derived ceramic (PDC) approach is a liquid based technique, it is non-line of sight and able to coat complex shapes.

SiCN ceramic coatings have been produced in multiple ways. Zeigmeister[1] used spray-coating method to make 50 μm-thick SiCN ceramic coating on C/C/SiC substrate; a dense and nearly crack-free coating is achieved by repeating the procedure 4 times. SiCN coatings have been proposed for wear, erosion or corrosion protection applications[2] as well as micro-electronic and optoelectronic devices.[3] Using a specially tailored ABSE polycarbosilazane solution as precursor for dip- and spray-coating techniques, Motz et al.[4] coated complex-shaped samples with a ceramic-like coating (at higher temperatures) that has good corrosion and thermal stabilities; moreover, the high flexibility of ABSE film also allows the coating of flexible metal foils. SiCN membranes (200–500 nm thick) can be spin-coated onto a porous Si_3N_4 substrate for hot gas separation applications due to their high temperature stability.[5] Iwamoto et al.[6] reported such a microporous amorphous membrane that exhibits hydrogen gas permeance of 1.3×10^{-8} mol/m^2 s Pa at 573 K and the selectivity ratio of H_2/N_2 at 141.

SiOC ceramic coatings are attractive because they can be used as thermal or environmental barrier coatings against harsh environments at elevated temperatures. Fukushima et al.[7] used transition metals as catalyst and alkoxysilane as precursor to

DOI of original article:10.1016/j.jeurceramsoc.2011.05.018.
* Corresponding author. Tel.: +1 206 685 8158; fax: +1 206 543 3100.
E-mail addresses: kshwang@u.washington.edu (K. Wang), martin.guenthner@uni-bayreuth.de (M. Günthner), guenter.motz@uni-bayreuth.de (G. Motz), bordia@u.washington.edu (R.K. Bordia).

0955-2219/$ – see front matter © 2011 Elsevier Ltd. All rights reserved.
doi:10.1016/j.jeurceramsoc.2011.05.047

produce SiOC coatings with a crack-free thickness of 0.2 mm after crosslinking; the material shows good flexibility and adhesion on several types of plastic substrates due to the high-T^3-ratio structure in the sol stage. Polysiloxanes have a natural advantage of making SiOC ceramic materials because of the incorporation of bonded oxygen in the backbone of the polymer. Blum et al.[8–11] developed a family of linear polysiloxane material, which can be crosslinked *in situ* at low temperature (150 °C) and converted to ceramics below 450 °C. Its suitable viscosity for the coating process and low cost (as a byproduct of the silicone industry) has made it an attractive precursor for this purpose. Torrey[12] used polyhydromethylsiloxane (PHMS) as matrix material to make a type of composite coatings with a tunable thickness of 10–30 μm; active fillers were added to compensate for the shrinkage of the polymer so that low-porosity and crack-free coatings can be formed. It was found that the coating layer can be chemically bonded to the metallic substrates after heat treatment and provide good oxidation protection.[13,14] Torrey and Bordia recently wrote a book chapter on the filler systems used in PDC bulk components and nano-composites,[15] while Scheffler and Torrey co-authored another chapter specifically on PDC coatings.[16]

However, there is lack of a study on the performance of active filler reinforced SiOC composite ceramic coatings in long term exposure to high temperature oxidizing environments. Torrey[12] reported a cyclic oxidation study on such coatings and found that all the samples survived ten consecutive cycles of heating (to 800 °C, one hour holding) and cooling (to room temperature, two hour holding) at 10 °C/min with no visible damage but increased coating density. This paper presents for the first time the results of 200-h static oxidation testing at 800 °C on these coatings, and the significant improvement due to a bond coat layer.

2. Experimental procedure

The metal substrate used in this study for PDC deposition was Inconel 617, a nickel-based superalloy. The metal plates were 30 mm long, 10 mm wide and 1.2 mm thick, polished to 1200 grit finish and cleaned using ultrasonication bath prior to processing.

$ZrSi_2$ submicron particles (Accumet Materials Co., Ossining, NY, USA) were used as active fillers and PHMS polymer (HMS-992, Gelest Inc., Morrisville, PA, USA) was the precursor for the matrix. The $ZrSi_2$ particles were attrition milled in isopropyl alcohol for 10 h at room temperature, dried at relatively low temperature (∼100 °C) in a convection drying oven, and ground back to fine powders using mortar and pestle. 30 vol.% of fillers were mixed with the required amount of PHMS (70 vol.%) and half of the required *n*-octane (98+%, Alfa Aesar, Ward Hill, MA, USA) solvent. By virtue of its low boiling point (126 °C) and low viscosity (∼1 centiPoise), *n*-octane was added to adjust the viscosity of the mixture to a range suitable for dip coating. The slurry was then ball-milled for 4 h in order to mix all the reactants well and remove agglomerates. 0.05 wt.% of $Ru_3(CO)_{12}$ (Alfa Aesar, Ward Hill, MA, USA) catalyst (to PHMS) was dissolved in the other half of *n*-octane, and the solution was added to the slurry, which would be ball-milled for another 30 min prior to dip coating. It formed the slurry with a final composition having a volume ratio of 3:5 between (filler + PHMS) and *n*-octane. The volume ratio of "filler to polymer" was determined using the calculated result of the method developed by Greil[17] for zero shrinkage pyrolysis of the composite system. The rheology of the slurry, which is mainly controlled by the amount of the solvent, is optimized to make coatings of the desired thickness, based on Torrey and Bordia's work.[18]

A mechanical testing frame, Instron 4505 (Illinois Tool Works Inc., Norwood, MA, USA), was used to dip coat slurries onto metallic alloy substrates. Dip coating took place under ambient conditions. Typical withdrawal speeds were between 100 and 1000 mm/min. Due to a long travelling distance (>20 mm) for the Instron crossbar, the substrate was assumed to move at a constant and accurate speed as programmed. The transition region of non-uniform coating thickness due to crossbar acceleration was estimated to be less than 1 mm.

Pyrolysis was performed in a tube furnace (CM-1200, CM Furnace Inc., Bloomfield, NJ, USA). Humid air was used for polymer's *in situ* crosslinking in the tube. The temperature profile had a 2 °C/min ramp rate for both heating and cooling processes. Temperature was held constant at 150 °C for 2 h for crosslinking, and at 800 °C for another 2 h for the pyrolysis of PHMS and oxidation of active fillers. This heating profile ensured that the ceramic matrix remained amorphous but fully converted, and filler particles could be highly oxidized.

For the pure silicon oxynitride (SiON) ceramic coating (used as bond coat), perhydropolysilazane PHPS NN 120-20 (a solution of 20 wt.% PHPS in dibutyl ether, Clariant Advanced Materials GmbH, Sulzbach, Germany) was used as the polymer precursor. PHPS is produced by ammonolysis of the dichlorosilane SiH_2Cl_2 and subsequent base-catalyzed dehydrogenative coupling.[19] Due to the large number of Si–H groups, PHPS is highly reactive with hydroxyl groups. Several studies have reported that PHPS polymer can be converted to a ceramic at temperatures as low as 50 °C in a high humidity environment (95%[20]) or with ceramic-transformation promoting agents, like NH_3, amine, acid compound or peroxide.[21] However, for high temperature applications, such as oxidation resistance, pyrolysis of the polymer is still the desirable route of converting PHPS to ceramic. Below 1000 °C, it is able to form silicon nitride if heat treated in inert atmosphere and SiON in air or oxygen atmosphere as reported by Günthner et al.[22] According to their thermogravimetric analysis results, PHPS was completely crosslinked around 150–200 °C. During crosslinking, there was no significant weight loss/gain. The main weight gain by incorporation of oxygen occurs in the 200–400 °C range despite the loss of ammonia and hydrogen. After 400 °C, the material does not have significant weight change, implying the completion of ceramic conversion.

Due to the viscosity of PHPS solution and the requirement of making crack-free coatings, a moderate withdrawal speed range was used: 100–500 mm/min, which would lead to thicknesses of pyrolyzed films around 0.5–1.5 μm. The coated samples were pyrolyzed at 800 °C. Pyrolysis was carried out in the same tube furnace aforementioned with both ends of the tube open to ensure that samples were always exposed to flowing air. Temperature

ramp rates of 2–3 °C/min were used for both heating and cooling cycles, while a typical holding time at pyrolysis temperature was 2 h. Once they were pyrolyzed, they were ready for subsequent processing or characterization.

The multi-layer coating system was made by dip-coating and pyrolyzing the SiON bond coat layer and the $ZrSi_2$-filled SiOC top coat layer in sequence. The experimental parameters have been described above.

In oxidation testings, weight gains of coated samples were measured by an analytical balance (RADWAG XA110 Intell-Lab Balance, sensitivity 0.01 mg, Váhy-RADWAG Company, Šumperk, Czech Republic). Microstructural evolution of coating samples at different stages of oxidation was observed using scanning electron microscopy, SEM (JSM-6000F, JEOL USA, Inc., Portland, OR).

3. Results and discussion

The primary objective of this study is to develop PDC coating systems that provide high level of oxidation protection to metallic systems at elevated temperatures. Three systems have been successfully made, which includes particle filled SiOC ceramic matrix composite coatings (from PHMS), SiON ceramic coatings (from PHPS) and a combined system of bond coat (SiON) and top coat (particle-filled SiOC) on metal substrates. They were tested under typical oxidizing environment (800 °C in air with ambient humidity ~30–50%) for long periods of time, i.e. 100 h and 200 h, in order to investigate their long term oxidation resistance. The two key parameters that were monitored during oxidation were the weight gain per unit area on a coating surface and the thickness of the thermally grown oxide (TGO) layers close to the ceramic–metal or ceramic–ceramic interface. The effectiveness of PDC coatings in protecting metal substrates is evaluated and discussed mainly on their abilities in keeping the integrity of the tested surface and their robustness during long-term use.

Prior to long-term oxidation tests, coating systems were pyrolyzed for only 2 h, and this may not necessarily lead to fully transformed and stable ceramic products. Therefore, the continuous weight gain of coating materials as powders were first studied. This experiment provided a baseline of weight gain in the coating system. SiON powder and $ZrSi_2$ particle-filled SiOC powder were taken from the pyrolysis of the same slurries that were used to make the coatings. The thermal profile during pyrolysis was the same as that for the coatings. The pyrolyzed powders were ground back to <75 μm using pestle and mortar. The oxidation tests on the powders were conducted at 800 °C in air for a total of 200 h with the weight gain measured at 50-h interval. The results are summarized in Table 1, and then plotted in Fig. 1.

In powders, SiON exhibits weight gain that linearly increases with time throughout the investigated time span, however, the oxidized amount is very small, i.e. ~0.16%, after 200-h oxidation at 800 °C. However, its weight gain during pyrolysis (from 336.22 mg to 347.67 mg, 3.4%) is significantly more. It is clear that SiON has almost reached its maximal oxidation potential within the first 2 h, dense passivating amorphous SiO_2 scale

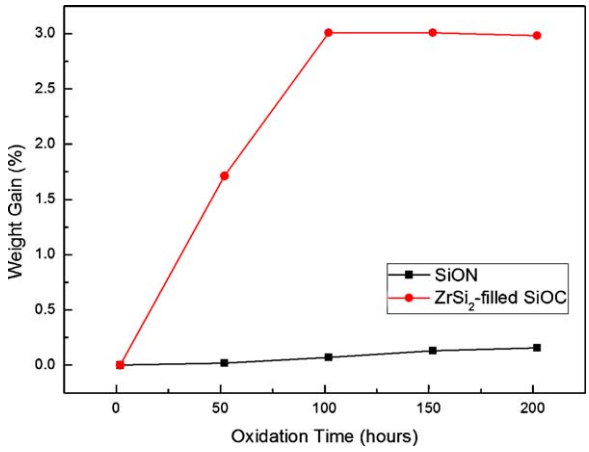

Fig. 1. Weight gain of SiON and 30 vol.% $ZrSi_2$-filled SiOC powders during 200-h oxidation at 800 °C.

forms on the particle surface. Therefore, oxidation after the completion of pyrolysis is limited. On the other hand, $ZrSi_2$-filled SiOC powder has a weight gain of about 3.5% (from 347.99 mg to 360.01 mg) during pyrolysis (2 h at 800 °C). However, it continues to oxidize linearly at a much higher rate (than that of SiON) for 100 h at 800 °C, then reaches a plateau value of approximately 3% weight gain for the second 100 h. These results are indicative of the differences in kinetics of the oxidation between SiON and $ZrSi_2$-filled SiOC powders. PHPS can be almost fully oxidized in 2 h at 800 °C, and is quite stable up to this temperature for at least 200 h. However, $ZrSi_2$-filled SiOC composite shows only half of its weight gain (3.5%) during the 2-h pyrolysis and the other half of its weight gain (3%) at a much slower rate, which takes about 100 h. This slow but continuous weight gain could be mainly attributed to the slow oxidation kinetics of $ZrSi_2$ particles, where the rate limiting step lies in the diffusion of oxygen to the reactive core through a growing outer oxide shell on top of each filler particles, which has been analyzed in the shrinking core model.[17]

Results on bulk powders mentioned above shed light on the oxidation mechanisms of different components in the ceramic coatings. However, they will not directly translate to the oxidation of the coatings, because of the size effect. For instance, the powders used in bulk tests were only milled to be on the 35–75 μm level, whereas the ceramic coatings are typically only 15 μm in the $ZrSi_2$-filled SiOC composite. Thus, the weight gain in the coating due to the oxidation of $ZrSi_2$ is expected to be at a faster rate than in the powder. The powder results should therefore be used as a conservative estimate of the expected weight gain in the coatings.

3.1. 100 h oxidation testing

Weight gains of the three coating systems: (a) particle filled SiOC ceramic matrix composite coatings (from PHMS); (b) SiON ceramic coatings (from PHPS); (c) combined system of bond coat (SiON) and top coat (SiOC + filler), were recorded before and after 100-h oxidation at 800 °C. Inconel 617 substrates (1200 grit surface finish) were used in this part of study.

Table 1
200-h oxidation of SiON and $ZrSi_2$-filled SiOC powders at 800 °C.

	SiON			30 vol.% $ZrSi_2$-filled SiOC		
	Net wt. (mg)	Δ wt. (mg)	Wt. gain (%)	Net wt. (mg)	Δ wt. (mg)	Wt. gain (%)
Before pyrolysis	336.22	N/A	N/A	347.99	N/A	N/A
After pyrolysis (2 h)	347.67	0	0	360.01	0	0
50 h	347.73	0.06	0.02	366.16	6.16	1.71
100 h	347.92	0.25	0.07	370.83	10.83	3.01
150 h	348.12	0.45	0.13	370.83	10.82	3.01
200 h	348.22	0.55	0.16	370.73	10.73	2.98

Table 2
100-h oxidation of the three PDC coating systems.

	Area (mm^2)	Weight gain (mg)	Normalized weight gain ($\mu g/mm^2$)
Bare Inconel 617	715.92	2.17	3.03
SiOC	606.84	0.97	1.59
SiON	584.56	0.63	1.08
SiON + SiOC	595.84	0.69	1.16

All three systems were pyrolyzed at 800 °C in air for 2 h. Numerical results are average values based on multiple samples and they are summarized in Table 2 and then plotted in Fig. 2.

Fig. 2 clearly shows that all PDC coating systems are able to effectively reduce the weight gain due to oxidation at elevated temperatures. When bare Inconel 617 metal substrates are exposed to the oxidation, they have a unit weight gain of roughly 3 $\mu g/mm^2$ after 100 h, however, this number is reduced to 1.59 $\mu g/mm^2$ for particle filled SiOC composite coatings, and to 1.08–1.16 $\mu g/mm^2$ for SiON coatings or (SiON + particle filled SiOC) coatings. Note that the weight gain in PDC coating samples includes not only the weight gain due to oxidation of the substrates, but also the weight gain in coatings themselves (proved in powder oxidation part). Taking this factor into account, the weight gain solely due to metal substrate can be further decreased. In other words, the performance of PDC coatings in reducing metal oxidation has been underestimated to a certain degree in the results shown here. For instance, in SiOC composite coatings, the withdrawal speed of 500 mm/min results in a final coating thickness of about 15 μm and the density of a similar system (the same polymer, PHMS, with the same volume fraction 70% in slurry) was measured to be 2.57 g/cm^3 after pyrolysis at 800 °C.[12] Therefore, in a unit area, 1 mm^2, the initial weight of the pyrolyzed SiOC composite coating is about 38.55 μg. The weight gain of the $ZrSi_2$-filled SiOC powder was 3.01% (see Table 1) after 100 h at 800 °C, hence, the SiOC composite coating gained weight as 1.16 $\mu g/mm^2$ by itself. The total weight gain of the composite coating measured on metal substrate is 1.59 $\mu g/mm^2$ in Table 2, of which only 0.43 $\mu g/mm^2$ should be attributed to the metal substrate oxidation. In this case, the oxidation of Inconel 617 substrates for 100 h is reduced from 3.03 $\mu g/mm^2$ to 0.43 $\mu g/mm^2$—a reduction of 86%.

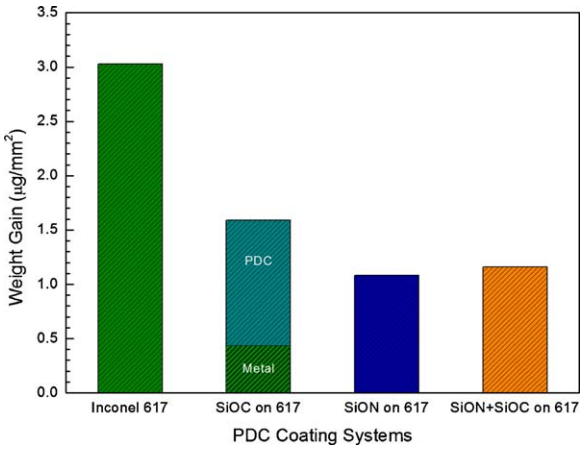

Fig. 2. Column graph of the normalized weight gains of the three PDC coating systems in 100-h oxidation.

Another important phenomenon in this experiment is that, with the addition of SiON bond coat, SiOC top coat has smaller weight gain than if it is used alone. The weight gain in SiON coatings on Inconel 617 is 1.08 $\mu g/mm^2$. It only increases to 1.16 $\mu g/mm^2$ with the addition of SiOC top coat, which is still considerably smaller than the value for only the SiOC coatings (1.59 $\mu g/mm^2$). In fact, the calculated weight gain within the SiOC composite coating layer (1.16 $\mu g/mm^2$) is equal to the total weight gain of the (SiON + particle filled SiOC) combined system measured on metal substrate (see Table 2). This implies that there is almost no oxidation of the Inconel 617 substrate in the 100-h test period. Hence, the combined SiON bond coat + particle filled SiOC top coat system provides almost complete oxidation protection for Inconel 617 at 800 °C, which will be proved again in the next section using another method.

3.2. 200 h oxidation testing

In order to further confirm the weight gain results in the previous section and the interpretation of a significant part of the weight gain coming from the coating itself, another method was used to investigate the effectiveness of the coating systems. We measured the thickness of the TGO layers that typically appear at the metal–ceramic interface. The three coating systems, described in the previous section, were oxidized for a longer time (200 h) at 800 °C with data collected every 50 h. Then, samples were sectioned in the thickness direction to reveal its cross section, using a low speed diamond saw. After polishing down to 0.05 μm (alumina suspension polishing media) finish and sputtered with platinum, the samples were

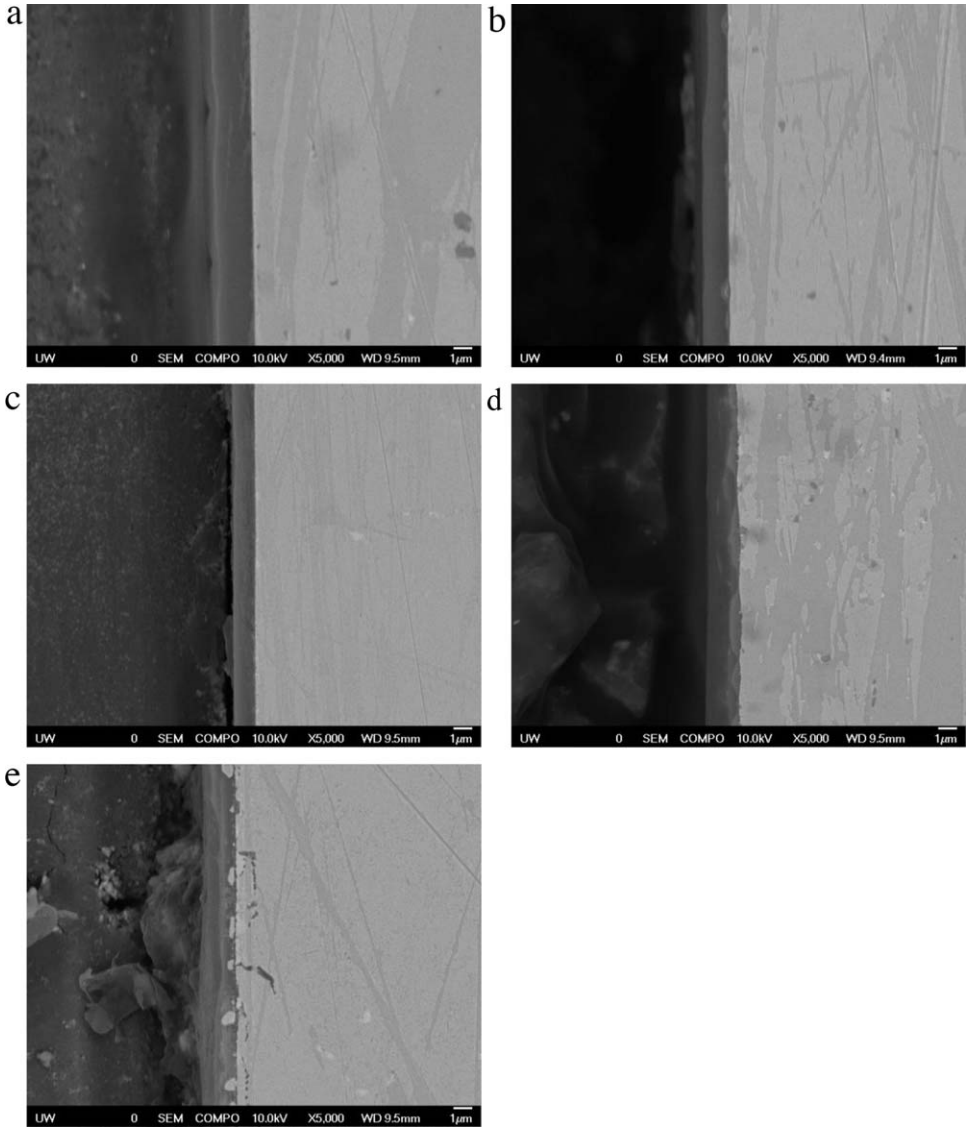

Fig. 3. Cross section backscattered SEM images of the SiON coating thermally oxidized at 800 °C for (a) 0 h; (b) 50 h; (c) 100 h; (d) 150 h; and (e) 200 h.

characterized with SEM in the backscattered mode. The micrographs of each sample in the three coating systems are shown in Figs. 3–5 respectively. The thicknesses of measured TGO layers in the $ZrSi_2$-filled SiOC coating system are listed in Table 3.

For SiON coatings, the average coating thickness is about 1.5 μm and the coatings are dense and amorphous from the beginning of the test (0 h) to the end (200 h). In the first 100 h, the TGO layer – a very thin layer lighter in colour than that of the bulk part of the coating – can be observed at the ceramic–metal interface. It is coherent and stable during this period of time. Estimated from a 10,000 × SEM micrograph (not shown), the thickness of this TGO layer is only ~0.15 μm, namely 1/10 of the total thickness. As shown in Fig. 3(d) and (e), the TGO layer has grown much thicker (nearly 1/3 of the total thickness) and more obvious in the last 100 h. The ceramic–metal interface is not as straight as before either, which is a clear sign of material degradation of the metal substrate. Especially in the 200-h sample (Fig. 3(e)), internal cracks can be seen to a depth of about 1 μm underneath the metal surface. There are some small pieces of metal debris present in the SiON coating close to the ceramic–metal interface. The reason for the debris formation is uncertain. Various possible explanations for these have been considered. The most likely reason appears to be the *in situ* formation of precipitates due to coalescence of diffused metal atoms. Other reasons, e.g. impurities introduced during processing, can be excluded since these are only observed in samples after long-term oxidation test. Further qual-

Table 3
TGO layer thickness in $ZrSi_2$-filled SiOC coatings.

Hours	TGO thickness (μm)
0	0.378 ± 0.084
50	0.751 ± 0.088
100	0.986 ± 0.111
150	1.248 ± 0.155
200	1.586 ± 0.130

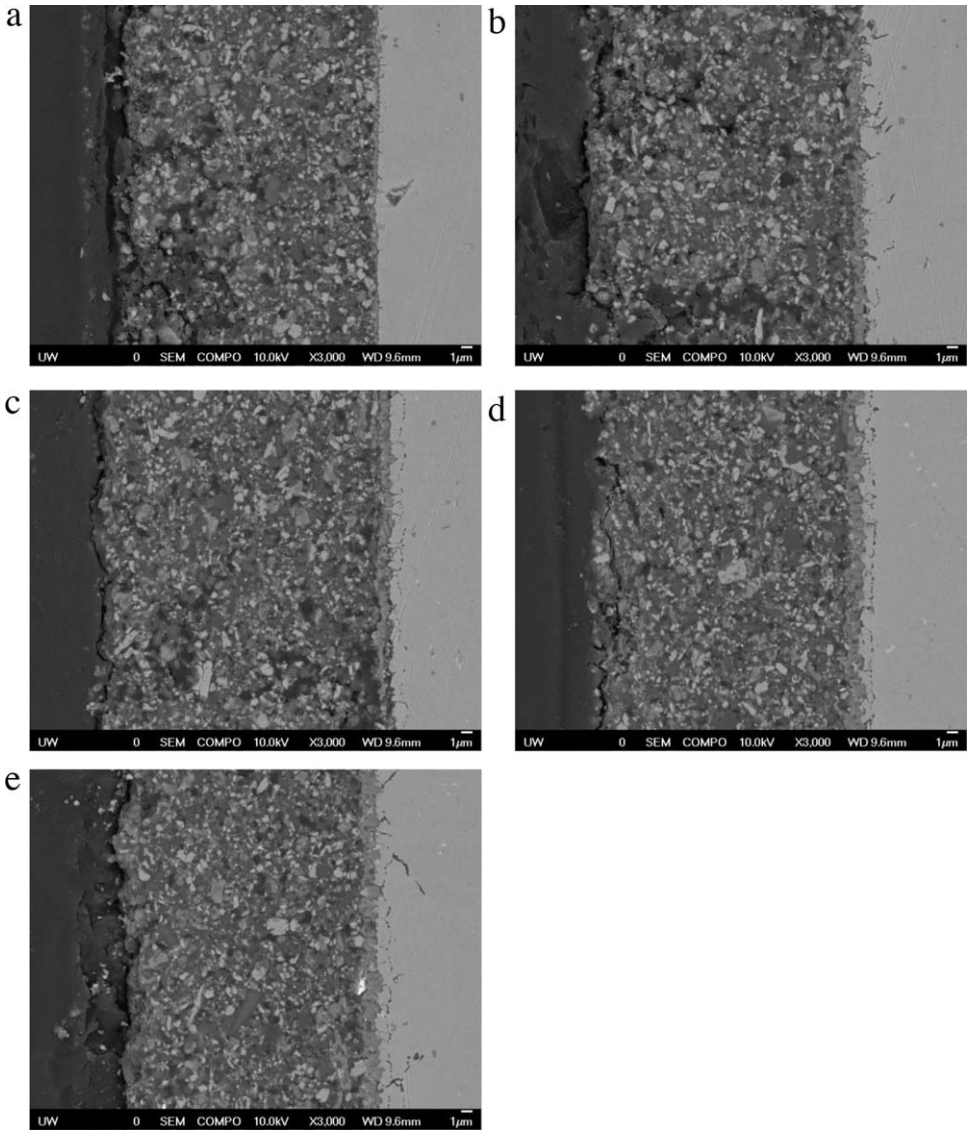

Fig. 4. Cross section backscattered SEM images of the $ZrSi_2$-filled SiOC coating thermally oxidized at 800 °C for (a) 0 h; (b) 50 h; (c) 100 h; (d) 150 h; and (e) 200 h.

itative investigation needs to be done to confirm their origin. Although starting to degrade, the PHPS coating is able to protect the metal substrate from oxidation up to 200 h at 800 °C. No major cracks can be observed either within the body of the coating itself or along the ceramic–metal interface. The cracks underneath the metal surface are minor at this point (200 h), but if the exposure is continued they will keep growing and eventually interconnect with each other to cause catastrophic failures.

For $ZrSi_2$-filled SiOC coatings, the coating thickness is about 20–25 μm in this section. It possesses the microstructure of a typical particle reinforced composite material with limited porosity. In terms of oxidation resistance performance, the more important features are the obvious growth of TGO layer at the ceramic–metal interface and the propagation of internal cracks roughly 1 μm underneath the metal surface. After coating pyrolysis, the TGO layer is only about 0.4 μm as shown in Fig. 4(a), but grows to be ~1.6 μm after 200 h. The measured TGO layer thickness is summarized in Table 3.

The correlation between TGO layer thickness and oxidation time is governed by a mixed form of parabolic relationship, which was first proposed by Evans[23,24] as follows Eq. (1):

$$x^2 + Ax = B(t + \tau) \tag{1}$$

$$A \equiv 2D_{eff}\left(\frac{1}{k} + \frac{1}{h}\right) \tag{1.a}$$

$$B \equiv \frac{2D_{eff}C^*}{N_1} \tag{1.b}$$

$$\tau \equiv \frac{x_0^2 + Ax_0}{B} \tag{1.c}$$

where x is oxide thickness at any given time, t is time, D_{eff} is the effective diffusion coefficient, k is solid-phase transport rate constant, h is gas-phase transport coefficient, C^* is the equilibrium concentration of the oxidant in the oxide, N_1 is the number of oxidant molecules incorporated into a unit volume of the oxide layer, x_0 is the initial oxide thickness at $t = 0$. The solution to

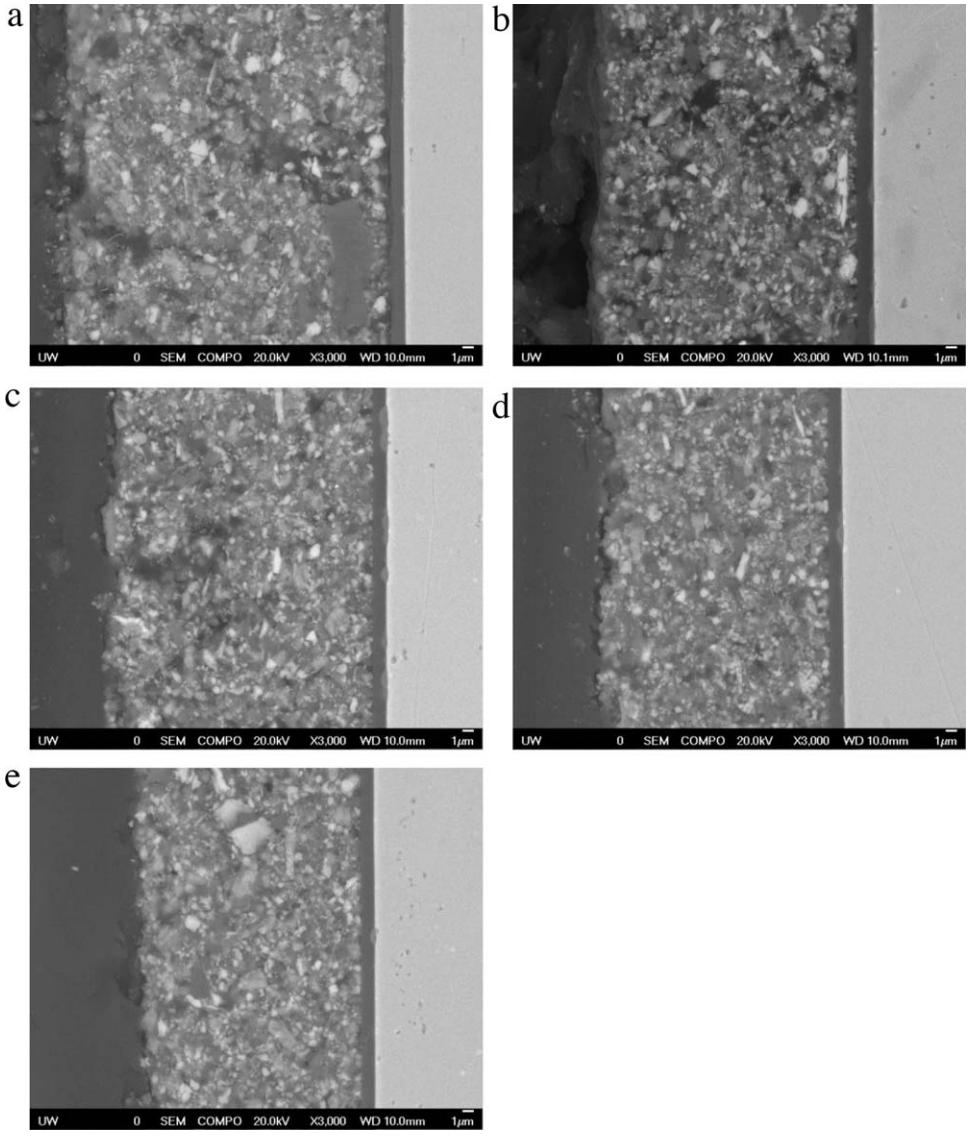

Fig. 5. Cross section backscattered SEM images of the combined SiON and $ZrSi_2$-filled SiOC coating thermally oxidized at 800 °C for (a) 0 h; (b) 50 h; (c) 100 h; (d) 150 h; and (e) 200 h.

Eq. (1), which yields the oxide thickness as a function of time, is stated below:

$$\frac{x}{A/2} = \left[1 + \frac{t+\tau}{A^2/4B}\right]^{1/2} - 1 \tag{2}$$

Simplified solutions for Eq. (2) under two limiting conditions have been proposed by Deal et al.[25] as follows:

When $t \gg A^2/4B$ and $t \gg \tau$,

$$\frac{x}{A/2} \cong \left(\frac{t}{A^2/4B}\right)^{1/2} \quad \text{or} \quad x^2 \cong Bt \tag{3}$$

When $t \ll A^2/4B$,

$$\frac{x}{A/2} \cong \frac{1}{2}\left(\frac{t+\tau}{A^2/4B}\right) \quad \text{or} \quad x \cong \frac{B}{A}(t+\tau) \tag{4}$$

For the long time scale investigated in this study, the form of Eq. (3) is appropriate. Fig. 6 is a plot of the TGO layer thickness, x^2, as a function of time. A linear fit is applied to the data set and indicates that Eq. (3) is valid. Data scatters around the fitting line in an acceptable range, revealing that the oxidation of $ZrSi_2$-filled PHMS coatings indeed follows the typical parabolic kinetics. The *parabolic rate constant B*, therefore, can be determined to be $B = 0.01134$ for this material system. The initial oxide thickness at hour = 0, measured to be 0.378 μm, is essentially due to the coating pyrolysis for 2 h. In the early stage of oxidation, oxide thickness has a linear relationship with time as shown in Eq. (4), and the rate constant (B/A) is much larger than parabolic rate constant B.

The real problem with this material system is evident from the internal cracks in the substrate that start to form as early as pyrolysis takes place. At 0 h, very small and short cracks vertical to the ceramic–metal interface can be observed at their initiation stage. After 50 h, they propagate deeper into the substrate,

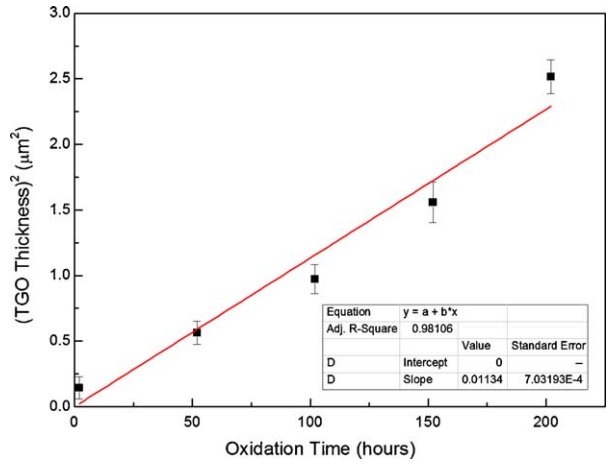

Fig. 6. A plot of the square of the TGO layer thickness as a function of thermal oxidation time at 800 °C.

meanwhile, voids start to form roughly on a plane parallel to the interface but about 1 μm underneath it. Between hour 100 and 200, these voids develop to a higher density. Once they become interconnected, major cracks that could either keep on that plane or deflect and kink out of the plane are present. Therefore, deep cracks into the substrate can be observed at 45° relative to the interface at hour 150 and 200. There were also the same type of internal cracks present in PHPS coatings, but they do not appear until after 150 h of oxidation. However, they form right after pyrolysis in the particle filled SiOC coating. This phenomenon is very closely depicted by Evans,[26] where the TGO layer cohesively bond with the ceramic but the metal fails in a ductile manner.

In fact, most ceramic–metal bonds are vulnerable to brittle debonding at the interface. However, in this study, the failure mode is different. From the microstructures, it is clear that the TGO layer and the SiOC coating are strongly bonded. The growth of the TGO layer is primarily facilitated by the active oxygen transported to this interface and the diffusion of metal atoms towards it. This diffusion is postulated to lead to the formation of the voids as shown in SEM micrographs. Thus, the interface fracture is mainly due to the nucleation, growth and coalescence of these voids. This mechanism was well studied by Evans et al.[26] as one of the four typical fracture mechanisms at metal–ceramic interfaces. Following the analysis presented in Ref. [26] the case in this study is a modified ductile fracture type with two additional factors: constraint and void nucleation. The constraint arises in this layered system with strong ceramic–metal bonds, where high hydrostatic stress builds up near the interface due to "inherent limitations on slip". The TGO layer is cohesively bonded: this is unlike a metal–metal interface, since metallic bonds allows certain degrees of slip without catastrophic plastic deformation. The presence of voids and cracks in this case is also a mechanism by which strain energy could be released and it is only governed by plastic dissipation. On the other hand, the number density of void nucleation sites is critical when the metal layer is thick, because the majority of the plastic dissipation is confined to the metal ligaments between the voids, which are favoured as the easiest path for the propagation of cracks parallel to the interface plane. Thus, the higher the void density, the lower the interface fracture resistance. As time progresses, more and more voids form due to unrelaxed stresses associated with the growth of the TGO layer, which eventually result in failure. Experimentally, delamination of SiOC coatings in small portions was observed during thermal oxidation, including in the early stage, since this fracture mechanism is more or less a local effect.

Experimentally, this problem seems to be solved by combining the two coating systems. The most important microstructural feature in the combined coating system in Fig. 5 is the elimination of TGO layers and thus the internal cracks in the metal. This should substantially improve the service life of metallic components. The proposed mechanism for this is the following. In the SiOC coatings, their open porosity is the diffusion path that oxygen can constantly and easily transport to the ceramic–metal interface and form the TGO layer. According to the parabolic relationship between oxidation time and TGO thickness, it takes long time for the TGO layer to reach its steady state-in fact this study has shown that steady state was not reached even after 200 h of oxidation. Thus, it is possible that catastrophic failure would occur in the SiOC coating before the equilibrium thickness of the TGO layer has been achieved. Therefore, to make robust oxidation resistant coatings from the PHMS system, it is important to block off the transport of oxygen to the metal surface. This can be achieved by the thin but dense SiON coating (∼1.5 μm), since dense SiO_x and Si_3N_4 are nearly impermeable to gas molecules like H_2O, O_2, N_2, Ar, Ke and Xe.[27] By itself, the thin SiON coating is a reasonable barrier to oxidation and for this case, internal cracks are not observed until 150 h. Ideally, to further improve SiON coating's service life, in other words, to further postpone the appearance of internal cracks, thicker coatings should be used, which requires repeating the dip-coating and pyrolysis process for multiple times. For instance, it needs about 14 times (∼1.5 μm per layer) for the SiON coating to reach 20 μm thick. However, thick SiOC top coat (∼20 μm) can be made in one step and it is more compliant than SiON coating of the same thickness due to its porosity and even lower Young's modulus. It is reasonable to assume that when the system is heated to 800 °C during operation the ceramic coating is nearly stress-free, because it was pyrolyzed at the same temperature. When cooling from high temperature to room temperature, due to its lower thermal expansion, the ceramic coating will be under compression as opposed to tension in the substrate. Thicker coatings tend to fail due to spallation under compressive stresses,[26] however, in this system it is possible to make thick coatings without failure, because the modulus and hence the stresses are low. A simple approximate calculation indicated that the magnitude of the maximum compressive stress, $(\sigma_C)_{compressive}$, in the coating at room temperature should be of the order of:

$$(\sigma_C)_{compressive} = E_C \Delta T(\alpha_M - \alpha_C) \quad (5)$$

in which C and M denote for ceramic and metal respectively, E is Young's modulus, ΔT is temperature difference between 800 °C and room temperature ($\Delta T = \sim 780$ °C), and α is CTE.

Table 4
Calculation of Young's modulus and stress in the "combined ceramic layer".

	E (GPa)	Thickness (h) (μm)	CTE (α) (K^{-1})
Substrate[28]	160	–	11.6×10^{-6}
Bond coat[29]	77.4	1.5	–
Top coat[29]	58.7	~20	1.0×10^{-6}
Combined ceramic layer	60.0	21.5	$\sim 1.0 \times 10^{-6}$

In Eq. (5), the effective modulus of the combined top and bond coat layer is given by:

$$E_{coating} \cong \frac{h_{bond} \cdot E_{bond} + h_{top} \cdot E_{top}}{h_{bond} + h_{top}} \quad (6)$$

Using the values in Table 4 for the modulus and the thickness, we can calculate the effective modulus to be 60 GPa.Substituting this in Eq. (5), together with values of $\alpha_M = 11.6 \times 10^{-6}\,K^{-1}$, $\alpha_C = 1.0 \times 10^{-6}\,K^{-1}$ (estimated value for the amorphous SiOC matrix), and $\Delta T = 780\,^{\circ}C$, we calculate the maximum compressive stress in the coating at room temperature to be approximately 496 MPa. Since the residual stresses in the coating are not only compressive but also relatively low, it is therefore able to survive temperature changes in this temperature range. Thus, the two coating systems complement each other if used together and result in a robust oxidation protection system.

The oxidation experiments on this combined system successfully proved this concept. The bond coat links the substrate and the top coat together via strong chemical bonding. As shown in Fig. 5, no reaction products are formed at the SiOC–SiON interface during the 200-h test; meanwhile, after 200 h, the TGO layer (<0.15 μm) at the SiON–metal interface is observed to be less than 1/10 of its thickness (~1.5 μm) in a 8000× SEM micrograph (not shown). By the end of oxidation at 200 h, the integrity of the metal is intact with no cracks visible. Thus, the metallic components protected by the combined PDC coating system have the potential for a long service life.

4. Conclusion

This paper summarizes the details of the processing of three coating systems designed to provide oxidation protection to metallic systems and the results of long term static oxidation tests. The three systems are all based on polymer derived ceramic coatings and are: SiON, $ZrSi_2$-filled SiOC and SiON bond coat + particle filled SiOC top coat. Significant reduction in weight gain of metal substrates due to oxidation was observed in the samples of all three coating systems. Further investigation of the TGO layer thickness reveals that the double-layer coating system, made of SiON bond coat and particle filled SiOC top coat, is the most effective in oxidation protection of Inconel 617 superalloy at 800 °C. No degradation in the coatings, the metal substrate or the interfaces was observed for times up to 200 h in air.

Acknowledgement

KW and RKB would like to acknowledge partial support for the research at University of Washington from US Air Force Office of Scientific Research (Grant No. FA95550-09-1-0633).

References

1. Zeigmeister U. *Development of a mechanical and oxidation protection for ceramic substrates*. Darmstadt, Germany: Diploma Thesis, Department of Materials and Earth Sciences, Darmstadt University of Technology; 2003.
2. Badzian A, Badzian T, Drawl WD, Roy R. Silicon carbonitride: a rival to cubic boron nitride. *Diamond Relat Mater* 1998;**7**(10):1519–25.
3. Zhang W, Zhang K, Wang B. Influence of temperature on the properties of SiCxNy:H films prepared by plasma-enhanced chemical vapour deposition. *Mater Sci Eng B* 1994;**26**(2–3):133–40.
4. Motz G, Kabelitz T, Ziegler G. Polymeric and ceramic-like SiCN coatings for protection of (light) metals against oxidation and corrosion. In: Mandal H, Ovecoglu L, editors. *Euro ceramics VIII, key engineering materials*. Trans Tech Publications Ltd.; 2004. p. 481–4.
5. Völger KW. *Ceramic materials through a nonoxidic sol–gel process*. Darmstadt, Germany: PhD Thesis, Department of Materials and Earth Sciences, Darmstadt University of Technology; 2002.
6. Iwamoto Y, Sato K, Kato T, Inada T, Kubo Y. A hydrogen-permselective amorphous silica membrane derived from polysilazane. *J Eur Ceram Soc* 2005;**25**(2–3):257–64.
7. Fukushima M, Yasuda E, Nakamura Y, Kita H, Kawabata H, Tanabe Y. Preparation of a transition metal containing polymethylsilsesquioxane hybrids and silicon oxycarbide ceramics – the fabrication of coating and self-supported films. *J Ceram Soc Jpn* 2005;**113**(1315):210–5.
8. Blum YD. Hydroxysiloxane precursors for ceramic manufacture. US Patent 5,128,494; 1992.
9. Blum YD, Johnson SM, Gusman MI. Hydridosiloxanes as precursors to ceramic products. US Patent 5,635,250; 1997.
10. Blum YD, MacQueen DB. Modifications of hydrosiloxane polymers for coating applications. *Surf Coat Int B: Coat Trans* 2001;**84**(1):27–33.
11. Blum YD, McDermott GA. Dehydrocoupling treatment and hydrosilylation of silicon-containing polymers, and compounds and articles produced thereby. US Patent 5,639,844; 1997.
12. Torrey JD. *Polymer derived ceramic composites as environmental barrier coatings on steel*. Seattle: PhD Thesis, Materials Science and Engineering, University of Washington; 2006.
13. Torrey JD, Bordia RK. Phase and microstructural evolution in polymer-derived composite systems and coatings. *J Mater Res* 2007;**22**(7):1959–66.
14. Torrey JD, Bordia RK. Mechanical properties of polymer-derived ceramic composite coatings on steel. *J Eur Ceram Soc* 2008;**28**(1):253–7.
15. Torrey JD, Bordia RK. Filler systems (bulk components and nanocomposites). In: Colombo P, et al., editors. *Polymer derived ceramics: from nano-structure to applications*. Lancaster, Pennsylvania, USA: DEStech Publications, Inc.; 2010. p. 329–39 [chapter 5.2].
16. Scheffler F, Torrey JD. Coatings. In: Colombo P, et al., editors. *Polymer derived ceramics: from nano-structure to applications*. Lancaster, Pennsylvania, USA: DEStech Publications, Inc.; 2010. p. 358–65 [chapter 5.4].
17. Greil P. Active-filler-controlled pyrolysis of preceramic polymers. *J Am Ceram Soc* 1995;**78**(4):835–48.
18. Torrey JD, Bordia RK. Processing of polymer-derived ceramic composite coatings on steel. *J Am Ceram Soc* 2008;**91**(1):41–5.
19. Seyferth D, Wiseman GH. High-yield synthesis of Si_3N_4/SiC ceramic materials by pyrolysis of a novel polyorganosilazane. *J Am Ceram Soc* 1984;**67**(7):C132–3.
20. Bauer F, Decker U, Dierdorf A, Ernst H, Heller R, Liebe H, et al. Preparation of moisture curable polysilazane coatings Part I. Elucidation of low temperature curing kinetics by FT-IR spectroscopy. *Prog Org Coat* 2005;**53**(3):183–90.

21. Shimizu Y, Matsuo H, Yamada K. Composition for forming ceramic material and process for producing ceramic material. US Patent 5,922,411; 1999.
22. Günthner M, Kraus T, Dierdorf A, Decker D, Krenkel W, Motz G. Advanced coatings on the basis of Si(C)N precursors for protection of steel against oxidation. *J Eur Ceram Soc* 2009;**29**(10):2061–8.
23. Evans UR. Relation between tarnishing and corrosion. *Trans Am Electrochem Soc* 1924;**46**:247–82.
24. Evans UR. *The corrosion and oxidation of metals: scientific principles and practical applications.*. New York, USA: St. Martin's Press Inc; 1960.
25. Deal BE, Grove AS. General relationship for the thermal oxidation of silicon. *J Appl Phys* 1965;**36**(12):3770–8.
26. Evans AG, Dalgleish BJ. The fracture-resistance of metal ceramic interfaces. *Acta Metall Mater* 1992;**40**:S295–306.
27. Barrer RM. *Diffusion in and through solids*. Cambridge, England: Cambridge University Press; 1941.
28. MatWeb of Automation Creations Inc. Special Metals INCONEL Alloy 617. Available from: http://www.matweb.com/search/datasheet.aspx?MatGUID=adf2123d8e494e75aef7417989ffea92.
29. Wang K. *Polymer derived ceramic and ceramic matrix composite coatings: processing, characterization and performance*. Seattle: PhD Thesis, Materials Science and Engineering, University of Washington; 2010.